mined by the Hodgkin-Huxley functions $\alpha_m(V)$ and $\beta_m(V)$ and appropriate combinatoric factors. State 4 is the open state. The transition to the inactivated state 5, however, is quite different from the inactivation process in the Hodgkin-Huxley model. Inactivation transitions to state 5 can only occur from states 2, 3, and 4, and the corresponding transition rates k_1, k_2, and k_3 are constants, independent of voltage. The deinactivation process occurs at the Hodgkin-Huxley rate $\alpha_h(V)$ from state 5 to state 3.

Figure 5.13 shows simulations of this Na^+ channel model. In contrast to the K^+ channel model shown in figure 5.12, this model does not reproduce exactly the results of the Hodgkin-Huxley model when large numbers of channels are summed. Nevertheless, the two models agree quite well, as seen in the lower right panel of figure 5.13. The agreement, despite the different mechanisms of inactivation, is due to the speed of the activation process for the Na^+ conductance. The inactivation rate function $\beta_h(V)$ in the Hodgkin-Huxley model has a sigmoidal form similar to the asymptotic activation function $m_\infty(V)$ (see equation 5.24). This is indicative of the actual dependence of inactivation on m and not V. However, the activation variable m of the Hodgkin-Huxley model reaches its voltage-dependent asymptotic value $m_\infty(V)$ so rapidly that it is difficult to distinguish inactivation processes that depend on m from those that depend on V. Differences between the two models are only apparent during a sub-millisecond time period while the conductance is activating. Experiments that can resolve this time scale support the channel model over the original Hodgkin-Huxley description.

5.8 Synaptic Conductances

Synaptic transmission at a spike-mediated chemical synapse begins when an action potential invades the presynaptic terminal and activates voltage-dependent Ca^{2+} channels leading to a rise in the concentration of Ca^{2+} within the terminal. This causes vesicles containing transmitter molecules to fuse with the cell membrane and release their contents into the synaptic cleft between the pre- and postsynaptic sides of the synapse. The transmitter molecules then diffuse across the cleft and bind to receptors on the postsynaptic neuron. Binding of transmitter molecules leads to the opening of ion channels that modify the conductance of the postsynaptic neuron, completing the transmission of the signal from one neuron to the other. Postsynaptic ion channels can be activated directly by binding to the transmitter, or indirectly when the transmitter binds to a distinct receptor that affects ion channels through an intracellular second-messenger signaling pathway.

As with a voltage-dependent conductance, a synaptic conductance can be written as the product of a maximal conductance and an open channel probability, $g_s = \overline{g}_s P$. The open probability for a synaptic conductance can be expressed as a product of two terms that reflect processes occurring on

synaptic open probability P_s

the pre- and postsynaptic sides of the synapse, $P = P_s P_{rel}$. The factor P_s is the probability that a postsynaptic channel opens given that the transmitter was released by the presynaptic terminal. Because there are typically many postsynaptic channels, this can also be taken as the fraction of channels opened by the transmitter.

transmitter release probability P_{rel}

P_{rel} is related to the probability that transmitter is released by the presynaptic terminal following the arrival of an action potential. This reflects the fact that transmitter release is a stochastic process. Release of transmitter at a presynaptic terminal does not necessarily occur every time an action potential arrives, and, conversely, spontaneous release can occur even in the absence of action potential induced depolarization. The interpretation of P_{rel} is a bit subtle because a synaptic connection between neurons may involve multiple anatomical synapses, and each of these may have multiple independent transmitter release sites. The factor P_{rel}, in our discussion, is the average of the release probabilities at each release site. If there are many release sites, the total amount of transmitter released by all the sites is proportional to P_{rel}. If there is a single release site, P_{rel} is the probability that it releases transmitter. We will restrict our discussion to these two interpretations of P_{rel}. For a modest number of release sites with widely varying release probabilities, the current we discuss only describes an average over multiple trials.

ionotropic synapse
metabotropic synapse

Synapses can exert their effects on the soma, dendrites, axon spike-initiation zone, or presynaptic terminals of their postsynaptic targets. There are two broad classes of synaptic conductances that are distinguished by whether the transmitter binds to the synaptic channel and activates it directly, or the transmitter binds to a distinct receptor that activates the conductance indirectly through an intracellular signaling pathway. The first class is called ionotropic and the second metabotropic. Ionotropic conductances activate and deactivate more rapidly than metabotropic conductances. Metabotropic receptors can, in addition to opening channels, cause long-lasting changes inside a neuron. They typically operate through pathways that involve G-protein mediated receptors and various intracellular signalling molecules known as second messengers. A large number of neuromodulators including serotonin, dopamine, norepinephrine, and acetylcholine can act through metabotropic receptors. These have a wide variety of important effects on the functioning of the nervous system.

glutamate, GABA

Glutamate and GABA (γ-aminobutyric acid) are the major excitatory and inhibitory transmitters in the brain. Both act ionotropically and metabotropically. The principal ionotropic receptor types for glutamate

AMPA, NMDA

are called AMPA and NMDA. Both AMPA and NMDA receptors produce mixed-cation conductances with reversal potentials around 0 mV. The AMPA current is fast activating and deactivating. The NMDA receptor is somewhat slower to activate and deactivates considerably more slowly. In addition, NMDA receptors have an unusual voltage dependence that we discuss in a later section, and are rather more permeable to Ca^{2+} than

AMPA receptors.

GABA activates two important inhibitory synaptic conductances in the brain. $GABA_A$ receptors produce a relatively fast ionotropic Cl^- conductance. $GABA_B$ receptors are metabotropic and act to produce a slower and longer lasting K^+ conductance. *$GABA_A$, $GABA_B$*

In addition to chemical synapses, neurons can be coupled through electrical synapses (gap junctions) that produce a synaptic current proportional to the difference between the pre- and postsynaptic membrane potentials. Some gap junctions rectify so that positive and negative current flow is not equal for potential differences of the same magnitude. *gap junctions*

The Postsynaptic Conductance

In a simple model of a directly activated receptor channel, the transmitter interacts with the channel through a binding reaction in which k transmitter molecules bind to a closed receptor and open it. In the reverse reaction, the transmitter molecules unbind from the receptor and it closes. These processes are analogous to the opening and closing involved in the gating of a voltage-dependent channel, and the same type of equation is used to describe how the open probability P_s changes with time,

$$\frac{dP_s}{dt} = \alpha_s(1 - P_s) - \beta_s P_s \,. \tag{5.27}$$

Here, β_s determines the closing rate of the channel and is usually assumed to be a constant. The opening rate, α_s, on the other hand, depends on the concentration of transmitter available for binding to the receptor. If the concentration of transmitter at the site of the synaptic channel is [transmitter], the probability of finding k transmitter molecules within binding range of the channel is proportional to [transmitter]^k, and α_s is some constant of proportionality times this factor.

When an action potential invades the presynaptic terminal, the transmitter concentration rises and α_s grows rapidly causing P_s to increase. Following the release of transmitter, diffusion out of the cleft, enzyme-mediated degradation, and presynaptic uptake mechanisms can all contribute to a rapid reduction of the transmitter concentration. This sets α_s to zero, and P_s follows suit by decaying exponentially with a time constant $1/\beta_s$. Typically, the time constant for channel closing is considerably larger than the opening time.

As a simple model of transmitter release, we assume that the transmitter concentration in the synaptic cleft rises extremely rapidly after vesicle release, remains at a high value for a period of duration T, and then falls rapidly to zero. Thus, the transmitter concentration is modeled as a square pulse. While the transmitter concentration is nonzero, α_s takes a constant value much greater that β_s, otherwise $\alpha_s = 0$. Suppose that vesicle release

occurs at time $t = 0$ and that the synaptic channel open probability takes the value $P_s(0)$ at this time. While the transmitter concentration in the cleft is nonzero, α_s is so much larger than β_s that we can ignore the term involving β_s in equation 5.27. Integrating equation 5.27 under this assumption, we find that

$$P_s(t) = 1 + (P_s(0) - 1)\exp(-\alpha_s t) \quad \text{for} \quad 0 \le t \le T\,. \tag{5.28}$$

The open probability takes its maximum value at time $t = T$ and then, for $t \ge T$, decays exponentially at a rate determined by the constant β_s,

$$P_s(t) = P_s(T)\exp(-\beta_s(t - T)) \quad \text{for} \quad t \ge T\,. \tag{5.29}$$

If $P_s(0) = 0$, as it will if there is no synaptic release immediately before the release at $t = 0$, equation 5.28 simplifies to $P_s(t) = 1 - \exp(-\alpha_s t)$ for $0 \le t \le T$, and this reaches a maximum value $P_{\max} = P_s(T) = 1 - \exp(-\alpha_s T)$. In terms of this parameter, a simple manipulation of equation 5.28 shows that we can write, in the general case,

$$P_s(T) = P_s(0) + P_{\max}(1 - P_s(0))\,. \tag{5.30}$$

Figure 5.14 shows a fit to a recorded postsynaptic current using this formalism. In this case, β_s was set to 0.19 ms^{-1}. The transmitter concentration was modeled as a square pulse of duration $T = 1$ ms during which $\alpha_s = 0.93$ ms^{-1}. Inverting these values, we find that the time constant determining the rapid rise seen in figure 5.14A is 0.9 ms, while the fall of the current is an exponential with a time constant of 5.26 ms.

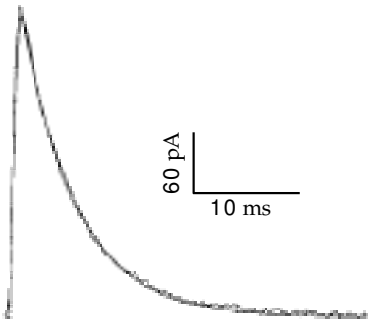

Figure 5.14: A fit of the model discussed in the text to the average EPSC (excitatory postsynaptic current) recorded from mossy fiber input to a CA3 pyramidal cell in a hippocampal slice preparation. The smooth line is the theoretical curve and the wiggly line is the result of averaging recordings from a number of trials. (Adapted from Destexhe et al., 1994.)

For a fast synapse like the one shown in figure 5.14, the rise of the conductance following a presynaptic action potential is so rapid that it can be approximated as instantaneous. In this case, the synaptic conductance

due to a single presynaptic action potential occurring at $t = 0$ is often written as an exponential, $P_s = P_{max} \exp(-t/\tau_s)$ (see the AMPA trace in figure 5.15A) where, from equation 5.29, $\tau_s = 1/\beta_s$. The synaptic conductance due to a sequence of action potentials at arbitrary times can be modeled by allowing P_s to decay exponentially to zero according to the equation

$$\tau_s \frac{dP_s}{dt} = -P_s \,, \tag{5.31}$$

and, on the basis of the equation 5.30, making the replacement

$$P_s \rightarrow P_s + P_{max}(1 - P_s) \tag{5.32}$$

immediately after each presynaptic action potential.

Equations 5.28 and 5.29 can also be used to model synapses with slower rise times, but other functional forms are often used. One way of describing both the rise and the fall of a synaptic conductance is to express P_s as the difference of two exponentials (see the $GABA_A$ and NMDA traces in figure 5.15). For an isolated presynaptic action potential occurring at $t = 0$, the synaptic conductance is written as

$$P_s = P_{max} B \left(\exp(-t/\tau_1) - \exp(-t/\tau_2) \right) \tag{5.33}$$

where $\tau_1 > \tau_2$, and B is a normalization factor that assures that the peak value of P_s is equal to one,

$$B = \left(\left(\frac{\tau_2}{\tau_1} \right)^{\tau_{rise}/\tau_1} - \left(\frac{\tau_2}{\tau_1} \right)^{\tau_{rise}/\tau_2} \right)^{-1} . \tag{5.34}$$

The rise time of the synapse is determined by $\tau_{rise} = \tau_1 \tau_2/(\tau_1 - \tau_2)$, while the fall time is set by τ_1. This conductance reaches its peak value $\tau_{rise} \ln(\tau_1/\tau_2)$ after the presynaptic action potential.

Another way of describing a synaptic conductance is to use the expression

$$P_s = \frac{P_{max} t}{\tau_s} \exp(1 - t/\tau_s) \tag{5.35}$$

for an isolated presynaptic release that occurs at time $t = 0$. This expression, called an alpha function, starts at zero, reaches its peak value at $t = \tau_s$, and then decays with a time constant τ_s. *alpha function*

We mentioned earlier in this chapter that NMDA receptor conductance has an additional dependence on the postsynaptic potential not normally seen in other conductances. To incorporate this dependence, the current due to the NMDA receptor can be described using an additional factor that depends on the postsynaptic potential, V. The NMDA current is written as $\overline{g}_{NMDA} G_{NMDA}(V) P (V - E_{NMDA})$. P is the usual open probability factor. The factor $G_{NMDA}(V)$ describes an extra voltage dependence due to the fact that, when the postsynaptic neuron is near its resting potential, *NMDA receptor*

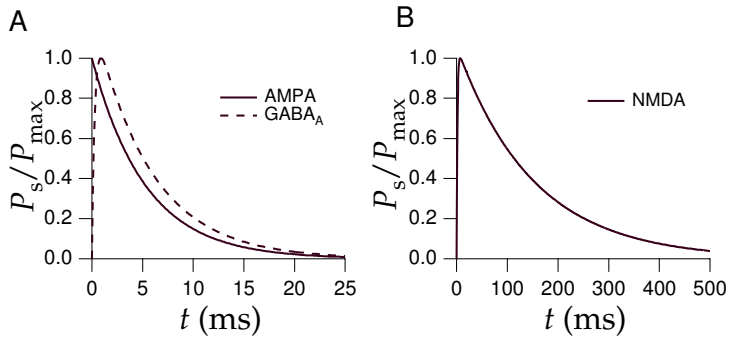

Figure 5.15: Time-dependent open probabilities fit to match AMPA, $GABA_A$, and NMDA synaptic conductances. A) The AMPA curve is a single exponential described by equation 5.31 with τ_s = 5.26 ms. The $GABA_A$ curve is a difference of exponentials with τ_1 = 5.6 ms and τ_{rise} = 0.3 ms. B) The NMDA curve is the differences of two exponentials with τ_1 = 152 ms and τ_{rise} = 1.5 ms. (Parameters are from Destexhe et al., 1994.)

NMDA receptors are blocked by Mg^{2+} ions. To activate the conductance, the postsynaptic neuron must be depolarized to knock out the blocking ions. Jahr and Stevens (1990) have fit this dependence by (figure 5.16)

$$G_{NMDA} = \left(1 + \frac{[Mg^{2+}]}{3.57\ \text{mM}} \exp(V/16.13\ \text{mV})\right)^{-1}. \tag{5.36}$$

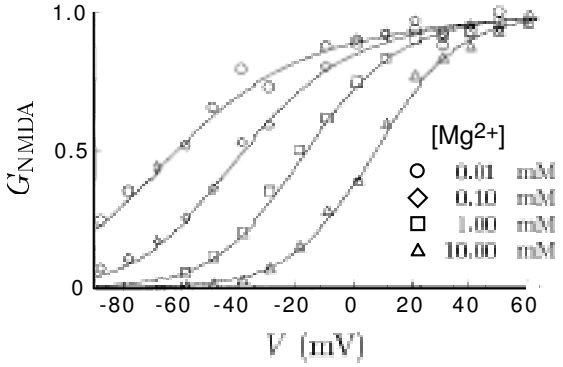

Figure 5.16: Dependence of the NMDA conductance on the extracellular Mg^{2+} concentration. Normal extracellular Mg^{2+} concentrations are in the range of 1 to 2 mM. The solid lines are the factors G_{NMDA} of equation 5.36 for different values of $[Mg^{2+}]$ and the symbols indicate the data points. (Adapted from Jahr and Stevens, 1990.)

NMDA receptors conduct Ca^{2+} ions as well as monovalent cations. Entry of Ca^{2+} ions through NMDA receptors is a critical event for long-term

modification of synaptic strength. The fact that the opening of NMDA receptor channels requires both pre- and postsynaptic depolarization means that they can act as coincidence detectors of simultaneous pre- and postsynaptic activity. This plays an important role in connection with the Hebb rule for synaptic modification discussed in chapter 8.

coincidence detection

Release Probability and Short-Term Plasticity

The probability of transmitter release and the magnitude of the resulting conductance change in the postsynaptic neuron can depend on the history of activity at a synapse. The effects of activity on synaptic conductances are termed short- and long-term. Short-term plasticity refers to a number of phenomena that affect the probability that a presynaptic action potential opens postsynaptic channels and that last anywhere from milliseconds to tens of seconds. The effects of long-term plasticity are extremely persistent, lasting, for example, as long as the preparation being studied can be kept alive. The modeling and implications of long-term plasticity are considered in chapter 8. Here we describe a simple way of describing short-term synaptic plasticity as a modification in the release probability for synaptic transmission. Short-term modifications of synaptic transmission can involve other mechanisms than merely changes in the probability of transmission, but for simplicity we absorb all these effects into a modification of the factor $P_{\rm rel}$ introduced previously. Thus, $P_{\rm rel}$ can be interpreted more generally as a presynaptic factor affecting synaptic transmission.

short-term plasticity

long-term plasticity

Figure 5.17 illustrates two principal types of short-term plasticity, depression and facilitation. Figure 5.17A shows trial-averaged postsynaptic current pulses produced in one cortical pyramidal neuron by evoking a regular series of action potentials in a second pyramidal neuron presynaptic to the first. The pulses decrease in amplitude dramatically upon repeated activation of the synaptic conductance, revealing short-term synaptic depression. Figure 5.17B shows a similar series of averaged postsynaptic current pulses recorded in a cortical inhibitory interneuron when a sequence of action potentials was evoked in a presynaptic pyramidal cell. In this case, the amplitude of the pulses increases, and thus the synapse facilitates. In general, synapses can exhibit facilitation and depression over a variety of time scales, and multiple components of short-term plasticity can be found at the same synapse. To keep the discussion simple, we consider synapses that exhibit either facilitation or depression described by a single time constant.

depression facilitation

Facilitation and depression can both be modeled as presynaptic processes that modify the probability of transmitter release. We describe them using a simple non-mechanistic model that has similarities to the model of $P_{\rm s}$ presented in the previous subsection. For both facilitation and depression, the release probability after a long period of presynaptic silence is $P_{\rm rel} = P_0$. Activity at the synapse causes $P_{\rm rel}$ to increase in the case of facilitation

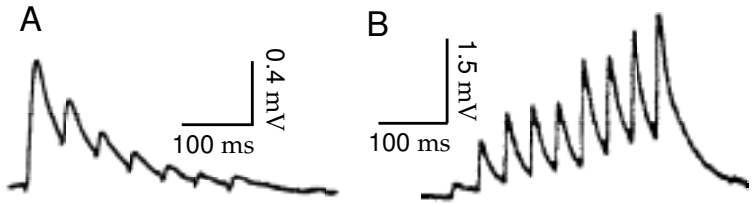

Figure 5.17: Depression and facilitation of excitatory intracortical synapses. A) Depression of an excitatory synapse between two layer 5 pyramidal cells recorded in a slice of rat somatosensory cortex. Spikes were evoked by current injection into the presynaptic neuron and postsynaptic currents were recorded with a second electrode. B) Facilitation of an excitatory synapse from a pyramidal neuron to an inhibitory interneuron in layer 2/3 of rat somatosensory cortex. (A from Markram and Tsodyks, 1996; B from Markram et al., 1998.)

and to decrease for depression. Between presynaptic action potentials, the release probability decays exponentially back to its 'resting' value P_0,

$$\tau_P \frac{dP_{rel}}{dt} = P_0 - P_{rel} \,. \tag{5.37}$$

The parameter τ_P controls the rate at which the release probability decays to P_0.

The models of facilitation and depression differ in how the release probability is changed by presynaptic activity. In the case of facilitation, P_{rel} is augmented by making the replacement $P_{rel} \to P_{rel} + f_F(1 - P_{rel})$ immediately after a presynaptic action potential (as in equation 5.32. The parameter f_F (with $0 \leq f_F \leq 1$) controls the degree of facilitation, and the factor $(1 - P_{rel})$ prevents the release probability from growing larger than one. To model depression, the release probability is reduced after a presynaptic action potential by making the replacement $P_{rel} \to f_D P_{rel}$. In this case, the parameter f_D (with $0 \leq f_D \leq 1$) controls the amount of depression, and the factor P_{rel} prevents the release probability from becoming negative.

We begin by analyzing the effects of facilitation on synaptic transmission for a presynaptic spike train with Poisson statistics. In particular, we compute the average release probability, denoted by $\langle P_{rel} \rangle$. $\langle P_{rel} \rangle$ is determined by requiring that the facilitation that occurs after each presynaptic action potential is exactly canceled by the average exponential decrement that occurs between presynaptic spikes. Consider two presynaptic action potentials separated by an interval τ, and suppose that the release probability takes its average value value $\langle P_{rel} \rangle$ at the time of the first spike. Immediately after this spike, it is augmented to $\langle P_{rel} \rangle + f_F(1 - \langle P_{rel} \rangle)$. By the time of the second spike, this will have decayed to $P_0 + (\langle P_{rel} \rangle + f_F(1 - \langle P_{rel} \rangle) - P_0) \exp(-\tau/\tau_P)$, which is obtained by integrating equation 5.37. The average value of the exponential decay factor in this expression is the integral over all positive τ values of $\exp(-\tau/\tau_P)$ times the probability density for a Poisson spike train with a firing rate r to produce an interspike inter-

val of duration τ, which is $r\exp(-r\tau)$ (see chapter 1). Thus, the average exponential decrement is

$$r\int_0^\infty d\tau\ \exp(-r\tau - \tau/\tau_P) = \frac{r\tau_P}{1+r\tau_P}\,. \tag{5.38}$$

In order for the release probability to return, on average, to its steady-state value between presynaptic spikes, we must therefore require that

$$\langle P_{rel}\rangle = P_0 + \left(\langle P_{rel}\rangle + f_F(1-\langle P_{rel}\rangle) - P_0\right)\frac{r\tau_P}{1+r\tau_P}\,. \tag{5.39}$$

Solving for $\langle P_{rel}\rangle$ gives

$$\langle P_{rel}\rangle = \frac{P_0 + f_F r\tau_P}{1+r f_F\tau_P}\,. \tag{5.40}$$

This equals P_0 at low rates and rises toward the value one at high rates (figure 5.18A). As a result, isolated spikes in low-frequency trains are transmitted with lower probability than spikes occurring within high-frequency bursts. The synaptic transmission rate when the presynaptic neuron is firing at rate r is the firing rate times the release probability. This grows linearly as $P_0 r$ for small rates and approaches r at high rates (figure 5.18A).

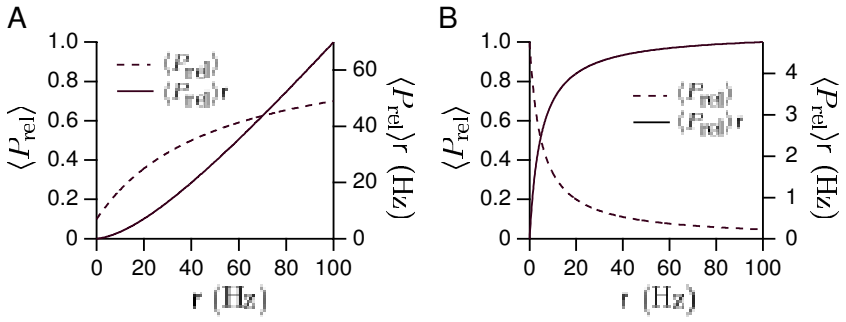

Figure 5.18: The effects of facilitation and depression on synaptic transmission. A) Release probability and transmission rate for a facilitating synapse as a function of the firing rate of a Poisson presynaptic spike train. The dashed curve shows the rise of the average release probability as the presynaptic rate increases. The solid curve is the average rate of transmission, which is the average release probability times the presynaptic firing rate. The parameters of the model are $P_0 = 0.1$, $f_F = 0.4$, and $\tau_P = 50$ ms. B) Same as A, but for the case of depression. The parameters of the model are $P_0 = 1$, $f_D = 0.4$, and $\tau_P = 500$ ms.

The value of $\langle P_{rel}\rangle$ for a Poisson presynaptic spike train can also be computed in the case of depression. The only difference from the above derivation is that following a presynaptic spike $\langle P_{rel}\rangle$ is decreased to $f_D\langle P_{rel}\rangle$. Thus, the consistency condition 5.39 is replaced by

$$\langle P_{rel}\rangle = P_0 + (f_D\langle P_{rel}\rangle - P_0)\frac{r\tau_P}{1+r\tau_P} \tag{5.41}$$

giving

$$\langle P_{\rm rel} \rangle = \frac{P_0}{1 + (1 - f_{\rm D}) {\rm r} \tau_{\rm P}} \tag{5.42}$$

This equals P_0 at low rates and goes to zero as $1/{\rm r}$ at high rates (figure 5.18B), which has some interesting consequences. As noted above, the average rate of successful synaptic transmissions is equal to $\langle P_{\rm rel} \rangle$ times the presynaptic rate r. Because $\langle P_{\rm rel} \rangle$ is proportional to $1/{\rm r}$ at high rates, the average transmission rate is independent of r in this range. This can be seen by the flattening of the solid curve in figure 5.18B. As a result, synapses that depress do not convey information about the values of constant, high presynaptic firing rates to their postsynaptic targets. The presynaptic firing rate at which transmission starts to become independent of r is around $1/((1 - f_{\rm D})\tau_{\rm P})$.

Figure 5.19 shows the average transmission rate, $\langle P_{\rm rel} \rangle {\rm r}$, in response to a series of steps in the presynaptic firing rate. Note first that the transmission rates during the 25, 100, 10 and 40 Hz periods are quite similar. This is a consequence of the $1/{\rm r}$ dependence of the average release probability, as discussed above. The largest transmission rates in the figure occur during the sharp upward transitions between different presynaptic rates. This illustrates the important point that depressing synapses amplify transient signals relative to steady-state inputs. The transients corresponding the 25 to 100 Hz transition and the 10 to 40 Hz transition are of roughly equal amplitudes, but the transient for the 10 to 40 Hz transition is broader than that for the 25 to 100 Hz transition.

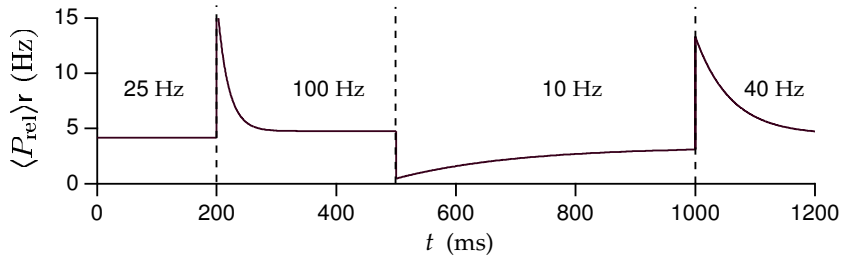

Figure 5.19: The average rate of transmission for a synapse with depression when the presynaptic firing rate changes in a sequence of steps. The firing rates were held constant at the values 25, 100, 10 and 40 Hz, except for abrupt changes at the times indicated by the dashed lines. The parameters of the model are $P_0 = 1$, $f_{\rm D} = 0.6$, and $\tau_{\rm P} = 500$ ms.

The equality of amplitudes of the two upward transients in figure 5.19 is a consequence of the $1/{\rm r}$ behavior of $\langle P_{\rm rel} \rangle$. Suppose that the presynaptic firing rate makes a sudden transition from a steady value r to a new value ${\rm r} + \Delta{\rm r}$. Before the transition, the average release probability is given by equation 5.42. Immediately after the transition, before the release probability has had time to adjust to the new input rate, the average transmis-

sion rate will be this previous value of $\langle P_{\rm rel} \rangle$ times the new rate $r + \Delta r$, which is $P_0(r + \Delta r)/(1 + (1 - f_D)r\tau_P)$. For sufficiently high rates, this is approximately proportional to $(r + \Delta r)/r$. The size of the change in the transmission rate is thus proportional to $\Delta r/r$, which means that depressing synapses not only amplify transient inputs, they transmit them in a scaled manner. The amplitude of the transient transmission rate is proportional to the fractional change, not the absolute change, in the presynaptic firing rate. The two transients seen in figure 5.19 have similar amplitudes because in both cases $\Delta r/r = 3$. The difference in the recovery time for the two upward transients in figure 5.19 is due to the fact that the effective time constant governing the recovery to a new steady-state level r is $\tau_P/(1 + (1 - f_D)\tau_P r)$.

5.9 Synapses On Integrate-and-Fire Neurons

Synaptic inputs can be incorporated into an integrate-and-fire model by including synaptic conductances in the membrane current appearing in equation 5.8,

$$\tau_m \frac{dV}{dt} = E_L - V - r_m \overline{g}_s P_s (V - E_s) + R_m I_e \,. \tag{5.43}$$

For simplicity, we assume that $P_{\rm rel} = 1$ in this example. The synaptic current is multiplied by r_m in equation 5.43 because equation 5.8 was multiplied by this factor. To model synaptic transmission, P_s changes whenever the presynaptic neuron fires an action potential using one of the schemes described previously.

Figures 5.20A and 5.20B show examples of two integrate-and-fire neurons driven by electrode currents and connected by identical excitatory or inhibitory synapses. The synaptic conductances in this example are described by the α function model. This means that the synaptic conductance a time t after the occurrence of a presynaptic action potential is given by $P_s = (t/\tau_s)\exp(-t/\tau_s)$. The figure shows a non-intuitive effect. When the synaptic time constant is sufficiently long (τ_s = 10 ms in this example), excitatory connections produce a state in which the two neurons fire alternately, out of phase with each other, while inhibitory synapses produce synchronous firing. It is normally assumed that excitation produces synchrony. Actually, inhibitory connections can be more effective in some cases than excitatory connections at synchronizing neuronal firing.

synchronous and asynchronous firing

Synapses have multiple effects on their postsynaptic targets. In equation 5.43, the term $r_m \overline{g}_s P_s E_s$ acts as a source of current to the neuron, while the term $r_m \overline{g}_s P_s V$ changes the membrane conductance. The effects of the latter term are referred to as shunting, and they can be identified most easily if

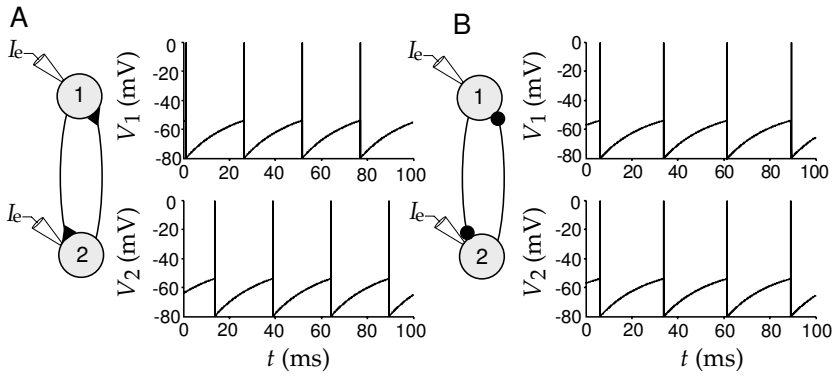

Figure 5.20: Two synaptically coupled integrate-and-fire neurons. A) Excitatory synapses (E_s = 0 mV) produce an alternating, out-of-phase pattern of firing. B) Inhibitory synapses (E_s = -80 mV) produce synchronous firing. Both model neurons have E_L = -70 mV, V_{th} = -54 mV, V_{reset} = -80 mV, $r_m\overline{g}_s$ = 0.05, P_{max} = 1, $R_m I_e$ = 25 mV, and τ_s = 10 ms.

we divide equation 5.43 by $1 + r_m\overline{g}_s P_s$ to obtain

$$\frac{\tau_m}{1 + r_m\overline{g}_s P_s}\frac{dV}{dt} = -V + \frac{E_L + r_m\overline{g}_s P_s E_s + R_m I_e}{1 + r_m\overline{g}_s P_s}. \tag{5.44}$$

The shunting effects of the synapse are seen in this equation as a decrease in the effective membrane time constant and a divisive reduction in the impact of the leakage and synaptic reversal potentials, and of the electrode current.

The shunting effects seen in equation 5.44 have been proposed as a possible basis for neural computations involving division. However, shunting only has a divisive effect on the membrane potential of an integrate-and-fire neuron; its effect on the firing rate is subtractive. To see this, assume that synaptic input is arriving at a sufficient rate to maintain a relatively constant value of P_s. In this case, shunting amounts to changing the value of the membrane resistance from R_m to $R_m/(1 + r_m\overline{g}_s P_s)$. Recalling equation 5.12 for the firing rate of the integrate-and-fire model and the fact that $\tau_m = C_m R_m$, we can write the firing rate in a form that reveals its dependence on R_m,

$$r_{isi} \approx \left[\frac{E_L - V_{th}}{C_m R_m (V_{th} - V_{reset})} + \frac{I_e}{C_m (V_{th} - V_{reset})}\right]_+. \tag{5.45}$$

Changing R_m only modifies the constant term in this equation, it has no effect on the dependence of the firing rate on I_e.

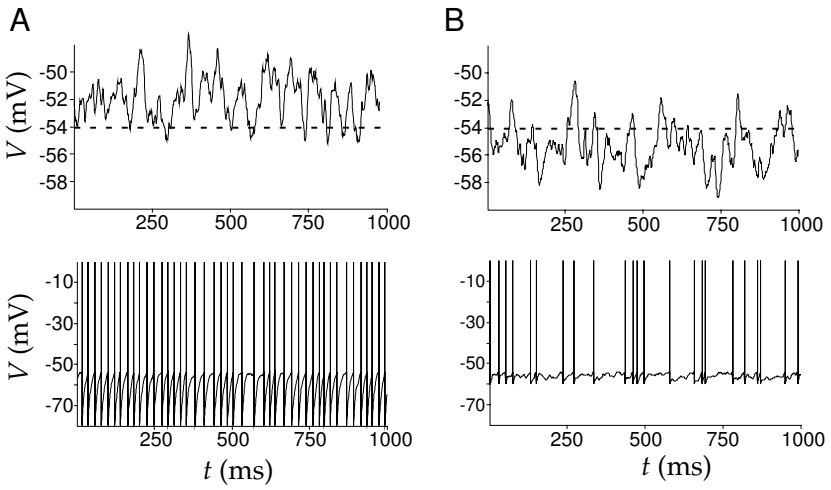

Figure 5.21: The regular and irregular firing modes of an integrate-and-fire model neuron. A) The regular firing mode. Upper panel: The membrane potential of the model neuron when the spike generation mechanism is turned off. The average membrane potential is above the spiking threshold (dashed line). Lower panel: When the spike generation mechanism is turned on, it produces a regular spiking pattern. B) The irregular firing mode. Upper panel: The membrane potential of the model neuron when the spike generation mechanism is turned off. The average membrane potential is below the spiking threshold (dashed line). Lower panel: When the spike generation mechanism is turned on, it produces an irregular spiking pattern. In order to keep the firing rates from differing too greatly between these two examples, the value of the reset voltage is higher in B than in A.

Regular and Irregular Firing Modes

Integrate-and-fire models are useful for studying how neurons sum large numbers of synaptic inputs and how networks of neurons interact. One issue that has received considerable attention is the degree of variability in the firing output of integrate-and-fire neurons receiving synaptic input. This work has led to the realization that neurons can respond to multiple synaptic inputs in two different modes of operation depending on the balance that exists between excitatory and inhibitory contributions.

The two modes of operation are illustrated in figure 5.21, which shows membrane potentials of an integrate-and-fire model neuron responding to 1000 excitatory and 200 inhibitory inputs. Each input consists of an independent Poisson spike train driving a synaptic conductance. The upper panels of figure 5.21 show the membrane potential with the action potential generation mechanism of the model turned off, and figures 5.21A and 5.21B illustrate the two different modes of operation. In figure 5.21A, the effect of the excitatory inputs is strong enough, relative to that of the inhibitory inputs, to make the average membrane potential, when action potential generation is blocked, more depolarized than the spiking thresh-

old of the model (the dashed line in the figure). When the action potential mechanism is turned on (lower panel of figure 5.21A), this produces a fairly regular pattern of action potentials.

The irregularity of a spike train can be quantified using the coefficient of variation (C_V), the ratio of the standard deviation to the mean of the interspike intervals (see chapter 1). For the Poisson inputs being used in this example, $C_V = 1$, while for the spike train in the lower panel of figure 5.21A, $C_V = 0.3$. Thus, the output spike train is much more regular than the input trains. This is not surprising, because the model neuron effectively averages its many synaptic inputs. In the regular firing mode, the total synaptic input attempts to charge the neuron above the threshold, but every time the potential reaches the threshold it gets reset and starts charging again. In this mode of operation, the timing of the action potentials is determined primarily by the charging rate of the cell, which is controlled by its membrane time constant.

Figure 5.21B shows the other mode of operation that produces an irregular firing pattern. In the irregular firing mode, the average membrane potential is more hyperpolarized than the threshold for action potential generation (upper panel of figure 5.21B). Action potentials are only generated when there is a fluctuation in the total synaptic input strong enough to make the membrane potential reach the threshold. This produces an irregular spike train, such as that seen in the lower panel of figure 5.21B which has a C_V value of 0.84.

The high degree of variability seen in the spiking patterns of *in vivo* recordings of cortical neurons (see chapter 1) suggests that they are better approximated by an integrate-and-fire model operating in an irregular-firing mode. There are advantages to operating in the irregular-firing mode that may compensate for its increased variability. One is that neurons firing in the irregular mode reflect in their outputs the temporal properties of fluctuations in their total synaptic input. In the regular firing mode, the timing of output spikes is only weakly related to the temporal character of the input spike trains. In addition, neurons operating in the irregular firing mode can respond more quickly to changes in presynaptic spiking patterns and firing rates than those operating in the regular firing mode.

5.10 Chapter Summary

In this chapter, we considered the basic electrical properties of neurons including their intracellular and membrane resistances, capacitances, and active voltage-dependent and synaptic conductances. We introduced the Nernst equation for equilibrium potentials and the formalism of Hodgkin and Huxley for describing persistent, transient, and hyperpolarization-activated conductances. Methods were introduced for modeling stochastic channel opening and stochastic synaptic transmission, including the

effects of synaptic facilitation and depression. We discussed a number of ways of describing synaptic conductances following the release of a neurotransmitter. Two models of action potential generation were discussed, the simple integrate-and-fire scheme and the more realistic Hodgkin-Huxley model.

5.11 Appendices

A) Integrating the Membrane Potential

We begin by considering the numerical integration of equation 5.8. It is convenient to rewrite this equation in the form

$$\tau_V \frac{dV}{dt} = V_\infty - V \,. \tag{5.46}$$

where $\tau_V = \tau_m$ and $V_\infty = E_\mathrm{L} + R_\mathrm{m} I_\mathrm{e}$. When the electrode current I_e is independent of time, the solution of this equation is

$$V(t) = V_\infty + (V(t_0) - V_\infty) \exp(-(t - t_0)/\tau_V) \tag{5.47}$$

where t_0 is any time prior to t and $V(t_0)$ is the value of V at time t_0. Equation 5.9 is a special case of this result with $t_0 = 0$.

If I_e depends on time, the solution 5.47 is not valid. An analytic solution can still be written down in this case, but it is not particularly useful except in special cases. Over a small enough time period Δt, we can approximate $I_\mathrm{e}(t)$ as constant and use the solution 5.47 to step from a time t to $t + \Delta t$. This requires replacing the variable t_0 in equation 5.47 with t and t with $t + \Delta t$ so that

$$V(t + \Delta t) = V_\infty + (V(t) - V_\infty) \exp(-\Delta t/\tau_V) \,. \tag{5.48}$$

This equation provides an updating rule for the numerical integration of equation 5.46. Provided that Δt is sufficiently small, repeated application of the update rule 5.48 provides an accurate way of determining the membrane potential. Furthermore, this method is stable because, if Δt is too large, it will only move V toward V_∞ and not, for example, make it grow without bound.

The equation for a general single-compartment conductance-based model, equation 5.6 with 5.5, can be written in the same form as equation 5.46 with

$$V_\infty = \frac{\sum_i g_i E_i + I_\mathrm{e}/A}{\sum_i g_i} \tag{5.49}$$

and

$$\tau_V = \frac{c_\mathrm{m}}{\sum_i g_i} \,. \tag{5.50}$$

Note that if c_m is in units of nF/mm^2 and the conductances are in the units μS/mm^2, τ_V comes out in ms units. Similarly, if the reversal potentials are given in units of mV, I_e is in nA, and A is in mm^2, V_∞ will be in mV units.

If we take the time interval Δt to be small enough so that the gating variables can be approximated as constant during this period, the membrane potential can again be integrated over one time step using equation 5.48. Of course, the gating variables are not fixed, so once V has been updated by this rule, the gating variables must be updated as well.

B) Integrating the Gating Variables

All the gating variables in a conductance-based model satisfy equations of the same form,

$$\tau_z \frac{dz}{dt} = z_\infty - z \tag{5.51}$$

where we use z to denote a generic variable. Note that this equation has the same form as equation 5.46, and it can be integrated in exactly the same way. We assume that Δt is sufficiently small so that V does not change appreciably over this time interval (and similarly $[Ca^{2+}]$ is approximated as constant over this interval if any of the conductances are Ca^{2+}-dependent). Then, τ_z and z_∞, which are functions of V (and possibly $[Ca^{2+}]$) can be treated as constants over this period and z can be updated by a rule identical to 5.48,

$$z(t + \Delta t) = z_\infty + (z(t) - z_\infty) \exp(-\Delta t/\tau_z). \tag{5.52}$$

An efficient integration scheme for conductance-based models is to alternate using rule (5.48) to update the membrane potential and rule (5.52) to update all the gating variables. It is important to alternate the updating of V with that of the gating variables, rather than doing them all simultaneously, as this keeps the method accurate to second order in Δt. If Ca^{2+}-dependent conductances are included, the intracellular Ca^{2+} concentration should be computed simultaneously with the membrane potential. By alternating the updating, we mean that the membrane potential is computed at times $0, \Delta t, 2\Delta t, \ldots$, while the gating variables are computed at times $\Delta t/2, 3\Delta t/2, 5\Delta t/2, \ldots$. A discussion of the second-order accuracy of this scheme is given in Mascagni and Sherman (1998).

5.12 Annotated Bibliography

Jack et al. (1975); **Tuckwell (1988)**; **Johnston & Wu (1995)**; **Koch & Segev (1998)**; **Koch (1998)** cover much of the material in this chapter and chapter 6. **Hille (1992)** provides a comprehensive treatment of ion channels.

Hodgkin & Huxley (1952) present the classic biophysical model of the action potential, and **Sakmann & Neher (1983)** describe patch clamp recording techniques allowing single channels to be studied electrophysiologically.

The integrate-and-fire model was introduced by Lapicque in 1907. **Destexhe et al. (1994)** describe kinetic models of both ion channels and short-term postsynaptic effects at synapses. Marom & Abbott (1994) show how the Na^+ channel model of Patlak (1991) can be reconciled with typical macroscopic conductance models. For a review of the spike-response model, the integrated version of the integrate-and-fire model, see **Gerstner (1998)**. Wang (1994) has analyzed a spike-rate adaptation similar to the one we presented, and Stevens & Zador (1998) introduce an integrate-and-fire model with time-dependent parameters.

The dynamic aspects of synaptic transmission are reviewed in **Magelby (1987)** and **Zucker (1989)**. Our presentation followed Abbott et al. (1997), Varela et al. (1997), and Tsodyks & Markram (1997). Wang & Rinzel (1992) noted that inhibitory synapses can synchronize coupled cells, and in our discussion we followed the treatment in Van Vreeswijk et al. (1994). Our analysis of the regular and irregular firing mode regimes of integrate-and-fire cells was based on Troyer & Miller (1997). Numerical methods for integrating the equations of neuron models are discussed in **Mascagni & Sherman (1998)**.